PHYSICAL REVIEW B **89**, 020508(R) (2014)

Effective thickness of two-dimensional superconductivity in a tunable triangular quantum well of $SrTiO_3$

K. Ueno,[1,2,*] T. Nojima,[3] S. Yonezawa,[4] M. Kawasaki,[5] Y. Iwasa,[5] and Y. Maeno[4]

[1]*Department of Basic Science, University of Tokyo, Tokyo 153-8902, Japan*

[2]*PRESTO, Japan Science and Technology Agency, Tokyo 102-0076, Japan*

[3]*Institute for Materials Research, Tohoku University, Sendai 980-8577, Japan*

[4]*Department of Physics, Graduate School of Science, Kyoto University, Kyoto 606-8502, Japan*

[5]*Quantum-Phase Electronics Center and Department of Applied Physics, University of Tokyo, Tokyo 113-8656, Japan, Center for Emergent Matter Science (CEMS), RIKEN, Wako 351-0198, Japan*

(Received 5 June 2013; revised manuscript received 8 January 2014; published 28 January 2014)

We report two-dimensionality and effective thickness of the superconductivity of a $SrTiO_3$ single-crystal surface induced by electric double-layer gating. The carrier density was tuned from 3×10^{13} to 1.1×10^{14} cm^{-2} by gating, where superconductivity appears with T_c of around 0.4 K. Typical two-dimensional behavior perfectly described by the Ginzburg–Landau equation was observed in the angular and temperature dependence of the upper critical magnetic field. The effective thickness of the superconducting layer remains nearly invariant, ranging from 11 to 13 nm, with increasing charge carrier density. This invariance contradicts the expected reduction in the thickness of the accumulation layer in a triangular quantum well model. This unexpected invariance of the superconducting layer thickness is probably a unique nature for a two-dimensional electron system in the incipient ferroelectric $SrTiO_3$.

DOI: 10.1103/PhysRevB.89.020508 PACS number(s): 73.20.−r, 73.40.−c, 74.78.Fk, 74.90.+n

I. INTRODUCTION

The effects of electric field on superconductors have attracted renewed interest because of the recent development of techniques to induce superconducting states in insulators and to tune superconducting properties in thin films [1–11]. Application of an electric field to the surface of a solid through a gate dielectric causes the accumulation of charge carriers, and may induce superconductivity when appropriate solids are chosen. However, such electric-field-induced superconductivity has been a long-standing challenge owing to the limited charge carrier density available with the conventional metal-insulator-semiconductor field-effect transistor (FET) configuration [1–3]. Recently, we broke the limit by introducing an electric double-layer transistor (EDLT), and successfully demonstrated its electric-field-induced superconductivity using insulating $SrTiO_3$, which was followed by a discovery of a new superconductor $KTaO_3$ employing an electric field effect [4,6]. These examples imply the high potential of EDLTs to control physical properties of materials, and at the same time raise fundamental questions concerning the nature of the electric-field-induced system, such as the dimensionality of superconductivity.

Thin-film superconductors behave as a two-dimensional (2D) system when the film thickness is less than the Ginzburg–Landau (GL) coherence length ξ_{GL}. In most case, two-dimensionality is characterized through the anisotropic upper critical magnetic field B_{c2}, which is described by the 2D GL equation [12]. Two-dimensional electron systems (2DES) on oxide heterostructures, such as δ-doped $SrTiO_3$, $LaAlO_3/SrTiO_3$, and $LaTiO_3/SrTiO_3$ interfaces, also show 2D superconductivity [13–16]. It has been reported that their superconducting layer thickness, which is experimentally deduced from the temperature dependence of B_{c2}, is estimated to be around 10 nm in common [13–16], although the origin of the similarity is an open question. Compared with these heterostructures, 2DES's in FET's or EDLT's induced by an electric field have good controllability, because the confinement potential of conduction carriers is tunable externally. It is known, in general, that the thickness/density of the carriers in the normal state is considered to decrease/increase with increasing gate bias, respectively [17]. However, it is not obvious whether the dimensionality of the superconducting state is controlled in a similar manner. Therefore the comparison of the effective thickness between the normal and superconducting states is crucial to obtain deeper understanding of electric-field-induced superconductivity.

In this study, we examined the two-dimensionality of electric-field-induced superconductivity on $SrTiO_3$ under various gate electric fields. The anisotropic B_{c2} for all electric fields follows the 2D GL theory for a homogeneous superconductor quite well. Detailed measurements indicate that the effective thickness of the superconducting layer is rather insensitive to the gate electric field (or the carrier density). This observed invariance of the thickness differs from an expected decrease of the thickness of 2DES in a conventional semiconductor. This result suggests that a simple triangular quantum well model is insufficient for describing 2DES on incipient ferroelectric $SrTiO_3$.

II. EXPERIMENT

An EDLT device as schematically illustrated in Fig. 1(a) was fabricated on a (001) surface of a single crystal of $SrTiO_3$. The fabrication procedure was reported in detail previously [18]. The conduction channel was rectangular with a width of 60 μm and length of 500 μm with many Au(100 nm)/Ti(20 nm) electrodes for transport measurements.

*ueno@phys.c.u-tokyo.ac.jp

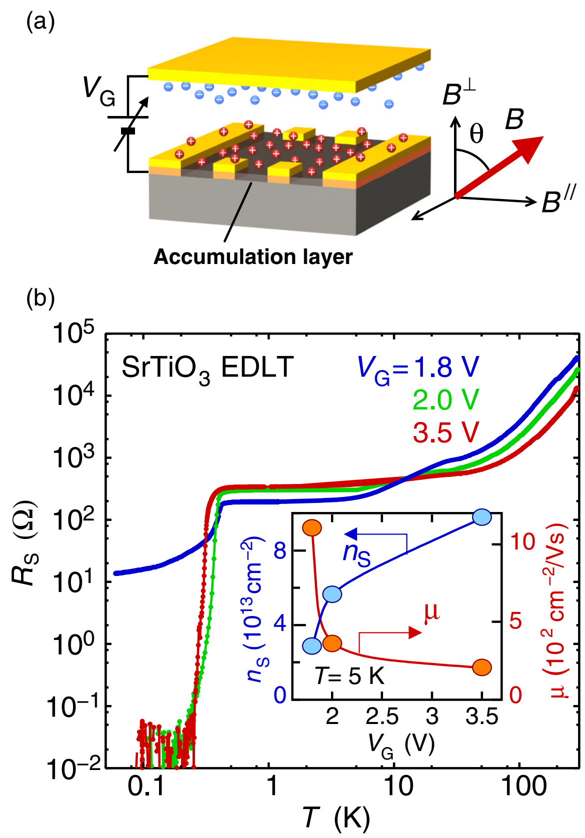

FIG. 1. (Color online) (a) Schematic illustration of the EDLT, where an electric double layer is formed by accumulated surface charges and cations (⊕). The definition of the magnetic field orientation θ is also shown. (b) Temperature dependence of sheet resistance R_S for various gate biases. (Inset) Variations of the sheet carrier density n_S and electron mobility μ with the gate voltage V_G at 5 K.

Polymer electrolyte with polyethylene oxide and $KClO_4$ was used as a gate dielectric. Transport properties were measured using a lock-in technique with alternating current (10 Hz) of 40 nA. The device was cooled in a dilution refrigerator (Kelvinox 25; Oxford Instruments), while the temperature T of the device was monitored by Pt and RuO_2 resistance thermometers for $T > 30$ K and $T < 5$ K, respectively. Magnetic field B up to 5 T was applied using a superconducting vector magnet system [19]. The angle θ between the normal of the interface and B, as shown in Fig. 1(a), was accurately determined within an error of 0.05° by making use of the anisotropy of the upper critical field B_{c2}. The Hall measurements to obtain sheet carrier density n_S were carried out around 200 K with a magnetic field perpendicular to the surface ranging from +1 to –1 T.

III. RESULTS AND DISCUSSION

Figure 1(b) shows the T dependence of the sheet resistance R_S in a magnetic field $B = 0$ T from room temperature to 0.08 K for the gate voltage V_G varying from 1.8 to 3.5 V. The R_S-T curves indicate metallic behavior with R_S decreasing by one or two orders of magnitude on cooling from room temperature to 5 K, followed by the superconducting transition. These curves are consistent with previous results obtained for the $SrTiO_3$ EDLT [4]. It is noted that R_S for $V_G = 3.5$ V becomes the largest at low temperatures (around 1–5 K), in spite of the increase in n_S with V_G. This anomalous behavior is attributed to the rapid decrease in the electron mobility μ at low temperature with increasing V_G in comparison with the increase in n_S.

Such a decrease in the low-temperature mobility μ with increasing V_G is explained in the following scenario. The high mobility of $SrTiO_3$ at low temperature originates from its large dielectric constant, which enhances the effective screening of Coulomb potentials of ionized impurity scattering [4,20]. Since undoped $SrTiO_3$ is an incipient ferroelectric, its dielectric constant is strongly dependent of the applied electric field. For example, application of a gate electric field of 20 kV/cm, which still is below our experimental range, suppresses the dielectric constant at low temperature by more than one order of magnitude [21]. This decrease not only enhances the carrier confinement, but also enhances impurity scattering through a reduction of screening. The combination of these effects drastically increases the probability of surface and impurity scattering of carriers, leading to a remarkable decrease in μ for larger V_G at low temperature as shown in the inset of Fig. 1(b), where μ is deduced from the Hall coefficient R_H and R_S at 5 K as $\mu = R_H/R_S$.

To estimate the quantitative length scale for the carrier confinement, we calculated the depth profiles of volume carrier density $n_V(z)$ against distance from the surface z. We used a quantum-well model with a triangular confinement potential $U(z)$. Figure 2 shows $U(z)$ and $n_V(z)$ for three V_G values considered in our experiments. As described in detail previously [4], we deduced $U(z)$ from the experimentally obtained n_S and the empirical relation of dielectric constant with E [21]. However, in our calculation, we assumed the dielectric constant to be independent of z and neglected the screening effect on $U(z)$. $n_S(z)$ and $n_V(z)$ were deduced by summing the squares of the occupied wave functions of subbands, which are a series of Airy functions as schematically

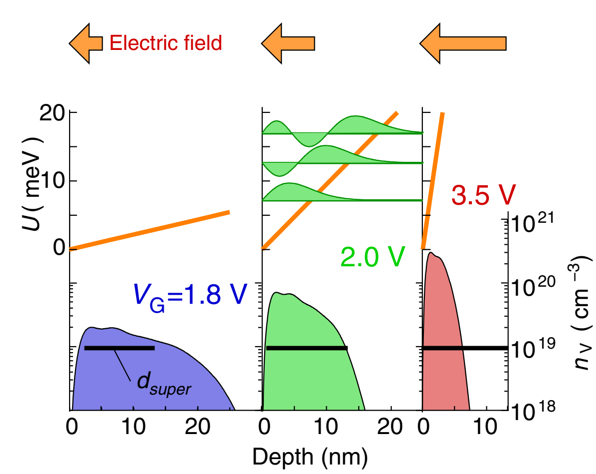

FIG. 2. (Color online) Depth dependence of the calculated carrier density n_V and confinement potential U for various gate voltage V_G. Length of horizontal bold lines in each V_G corresponds to d_{super}. A schematic illustration of three subband wave functions in a triangular quantum well is also shown in the top panel for $V_G = 2.0$ V.

RAPID COMMUNICATIONS

shown at the top of Fig. 2. As expected, we obtain the enhancement of carrier confinement with a bell-shaped $n_V(z)$ with increasing V_G, which is consistent with the decrease of the mobility shown in Fig. 1(b). The mean thickness of the accumulated layer in the normal state d_{normal} is defined as $n_S = d_{normal}\langle n_V\rangle$ with $\langle n_V\rangle = \int n_V^2(z)dz/\int n_V(z')dz'$, which is almost the same as the a full width of a half maximum of $n_V(z)$ for the bell-shaped distribution. We obtain d_{normal} of 20, 11, and 4.4 nm for $V_G = 1.8$, 2.0, and 3.5 V, respectively.

Below 1 K, $R_S(T)$ for $V_G = 2.0$ and 3.5 V exhibits a sharp superconducting transition to zero resistance. The critical temperatures T_c determined from the midpoint of the resistance drop are 0.39 and 0.34 K for $V_G = 2.0$ and 3.5 V, respectively. For V_G of 1.8 V, resistance dropped sharply with $T_c = 0.39$ K, but a finite resistance remained at low temperature. Since the resistance returned to the value at 1 K by applying a magnetic field or by increasing the current density, the transition for $V_G = 1.8$ V is also assigned to a superconducting transition. Finite residual resistance for the low carrier density has been reported previously [4].

To ascertain the 2D nature of the superconducting layer, we investigated the anisotropy of the upper critical magnetic field B_{c2} by measuring the T and B dependence of R_S. Figures 3(a) and 3(b) show typical R_S-T curves below 1 K for $V_G = 3.5$ V and B perpendicular ($\theta = 90°$) and parallel ($\theta = 0°$) to the conducting plane, respectively. The superconducting transition was entirely suppressed by B below 0.2 T and 1.6 T for $\theta = 90°$ and $\theta = 0°$, respectively, indicating strong anisotropy. In Fig. 3(c), $T_c(B)$ and $B_{c2}(T)$ defined as the midpoint of the resistance drop are plotted in the B-T plane to form $B_{c2}^{\perp}(T)$ and $B_{c2}^{//}(T)$ lines for the perpendicular and parallel conditions. The relationships, $B_{c2}^{\perp}(T) = B_{c2}^{\perp}(0)(1 - T/T_c)$ and $B_{c2}^{//}(T) = B_{c2}^{//}(0)(1 - T/T_c)^{1/2}$ around T_c, expected for 2D superconducting films, are confirmed as shown by the solid curves in Fig. 3(c). Furthermore, as shown in Fig. 3(d), the angular dependence of B_{c2} has a sharp cusp at $\theta = 90°$ and is precisely reproduced by Tinkham's formula [13]:

$$\left[\frac{B_{c2}(\theta)\cos\theta}{B_{c2}^{//}}\right]^2 + \left|\frac{B_{c2}(\theta)\sin\theta}{B_{c2}^{\perp}}\right| = 1, \qquad (1)$$

which is a solution to the 2D GL equation. The blue line in the inset of Fig. 3(d) corresponds to a theoretical curve obtained with a three-dimensional (3D) anisotropic GL (effective mass) model, which clearly fails to reproduce the experimental data particularly around $\theta = 90°$. Similar sets of data for $B_{c2}(T)$ and $B_{c2}(\theta)$, which agree with the 2D GL equation, were obtained for $V_G = 2.0$ and 1.8 V. Therefore we concluded that the electronic system in the electric-field-induced accumulation layer transforms into an "ideal" 2D superconductor. This seems to be a natural result of the 2D electron system. However, the electric-field-induced system has a complex subband structure with depth distribution in carrier density (see Fig. 2), and is completely different from simple metal thin films. Therefore the ideal 2D superconductivity in the electric-field-induced system may give us key information that is crucial for us to understand the peculiar feature of this system. It is noted that B_{c2} for the in-plane magnetic field exceeds the Pauli paramagnetic limit given by $\mu_0 H_P \sim 1.84\ T_c \sim 0.7$ T for

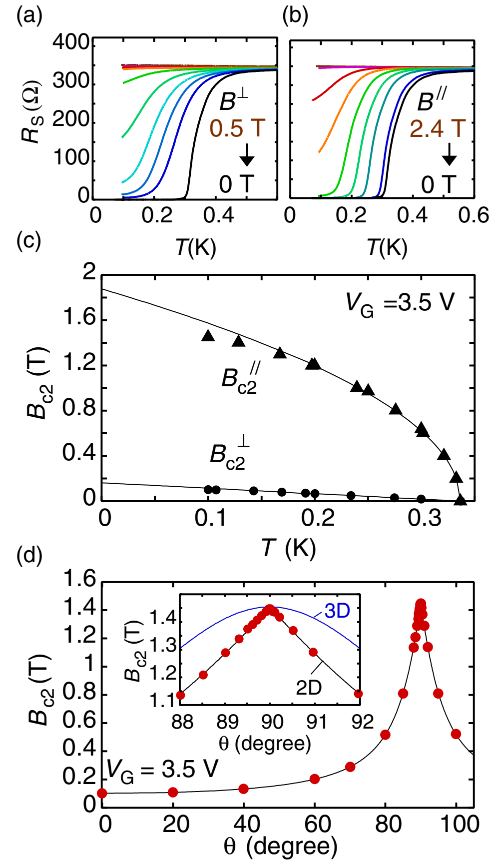

FIG. 3. (Color online) Temperature dependence of sheet resistance R_S around the superconducting transition for magnetic fields (a) perpendicular and (b) parallel to the surface. The values of magnetic fields from the bottom are 0, 0.03, 0.05, 0.07, 0.10, 0.15, 0.20, 0.22, 0.25, and 0.5 T for (a) and 0, 0.4, 0.8, 1.0, 1.2, 1.4, 1.6, 2.0, and 2.4 T for (b). (c) Temperature dependence of the upper critical magnetic field B_{c2} perpendicular and parallel to the surface, $B_{c2}^{\perp}(T)$ and $B_{c2}^{//}(T)$. Solid curves correspond to theoretical curves obtained from the 2D GL equation. (d) Angular dependence of B_{c2} at 0.1 K for $V_G = 3.5$ V. The inset shows magnification around $\theta = 90°$ (parallel to the surface). Black and blue solid curves correspond to theoretical ones obtained from Tinkham's 2D formula and the 3D effective mass model, respectively.

a BCS superconductor [22]. This indicates that the spin-orbit interaction, originating from the strong electric field at the surface, is strong enough to suppress Pauli paramagnetism.

From the fitting curves in Fig. 3(c), we deduced $B_{c2}^{\perp}(0)$ and $B_{c2}^{//}(0)$ for various V_G. We also deduced the GL coherence length at 0 K $\xi_{GL}(0)$ and the thickness of the superconducting layer d_{super} using the relations $B_{c2}^{\perp}(0) = \Phi_0/[2\pi\xi_{GL}^2(0)]$ and $B_{c2}^{//}(0) = \sqrt{12}\Phi_0/[2\pi d_{super}\xi_{GL}(0)]$, where Φ_0 is the magnetic flux quantum. Figure 4 shows $\xi_{GL}(0)$ and d_{super} against n_S together with the mean thickness of the accumulation layer in the normal state d_{normal} calculated from $n_V(z)$ in Fig. 2. Both $B_c^{\perp}(0)$ and $B_c^{//}(0)$ weakly depend on the gate bias with a maximum at $V_G = 2.0$ V ($n_S = 6 \times 10^{13}$ cm^{-2}). $\xi_{GL}(0)$ also weakly depends on n_S with a minimum at $V_G = 2.0$ V. The obtained $\xi_{GL}(0) = 45$–50 nm is four or five times larger than d_{super} for all values of n_S, which is consistent

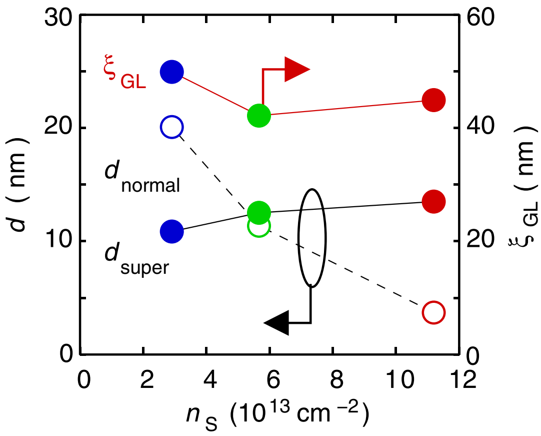

FIG. 4. (Color online) Sheet carrier density n_S dependence of the superconducting layer thickness d_{super}, the calculated mean thickness d_{normal}, and the GL coherence length $\xi_{GL}(0)$.

with the 2D behavior of the superconductivity. d_{super} shows a slight increase from 11 to 13 nm with increasing n_S. d_{super} is almost same as d_{normal} for V_G of 2.0 V, and is similar to the superconducting layer thickness for oxide heterostructures on $SrTiO_3$ [13–16].

The invariant $T_c \sim 0.3$–0.4 K against V_G or n_S in EDLTs of $SrTiO_3$ [4] has been recognized as a peculiar feature in contrast with the domelike dependence observed in a bulk $SrTiO_3$ [23] and other electric-field-tuned systems, such as $KTaO_3$ [6], MoS_2 [10], and the $LaAlO_3/SrTiO_3$ interface [3]. In addition, V_G dependence of d_{super} has never been experimentally examined in the electric-field-tuned systems. In this work, we succeed in reproducing this peculiarity and furthermore find that d_{super} is almost independent of V_G. These V_G-independent parameters may be closely related to each other.

The almost independent d_{super} of V_G is opposed to the expected decrease in d_{normal} from 20 nm to 4.4 nm. We now discuss the origin of the difference between the measured d_{super} and the calculated d_{normal}. Three possible scenarios are given: (1) a carrier distribution change during the superconducting transition, (2) inaccurate calculation of the carrier distribution, and (3) a narrower superconducting region than the whole carrier doped region. In the scenario (1), the carrier distribution and the effective thickness are assumed to change actually through the superconducting transition. As shown in Fig. 2, charge carriers are confined with an energy barrier of the order of 10 meV, which is much larger than the superconducting condensation energy of $\sim$50 μeV. Therefore it is unlikely that superconducting transition brings about the redistribution of carriers. The scenario (2) is based on the concern that our calculation of the carrier distribution is not sufficiently accurate, leading to a less reliable estimation of d_{normal}. Although the calculation of $n_V(z)$ presented in Fig. 2 assumes linear $U(z)$, we have to take account of nonlinearity of $U(z)$ for calculation of $n_V(z)$ due to z dependence of electric field E and dielectric constant ε. A screening effect due to induced carriers would reduce E and the slope of $U(z)$ with increasing z, resulting in a broader depth distribution. Indeed, Y. Mizohata *et al.* reported a broader depth distribution based on a microscopic theory with a consideration of the screening effect [24]. In addition, because of the incipient ferroelectricity in $SrTiO_3$, ε should also strongly depend on z through the $E(z)$ dependence of ε. As a result, ε at the interface is several orders of magnitude smaller than that in the bulk. This results in stronger confinement of carriers at around the interface. We consider that the combination of these two effects with opposite directions weakens the V_G dependence of $n(z)$ and d_{normal}. Therefore more accurate calculation of d_{normal} with the nonlinear $U(z)$ is necessary for comparison with the V_G independent d_{super}. In the scenario (3), superconductivity is assumed to emerge only in a part of the conductive layer. 2DES on $SrTiO_3$ has a bell-shaped depth dependence of carrier density. Chemically doped $SrTiO_3$ shows superconductivity for carrier density above a certain threshold n_{th} [23]. Then, it is likely that the part of carrier doped region with $n_V(z)$ above n_{th} shows superconductivity. In this situation, superconductivity emerges only in the center of the conductive layer. Bold lines in Fig. 2 indicate length of d_{super} in the $n(z)$ plot. For V_G of 1.8 and 2.0 V, d_{super} is identical to the thickness of the central region where $n(z) > n_{th}$ with n_{th} of 10^{19}cm^{-3}. For V_G of 3.5 V, the thickness of the central region is smaller than d_{super}. However, from scenario (2), the nonlinearity of $U(z)$ results in a broader distribution in bulk region. Therefore, combining with scenario (2), the thickness of the central region where $n(z) > n_{th}$ would increase for V_G of 3.5 V due to large n_S. We consider that the combination of scenarios (2) and (3) may give a consistent value of the superconducting layer with the experimental d_{super}.

Furthermore, we would like to point out that the GL equation assumes an isotropic superconductor that has a constant superconducting critical parameter in the depth direction. In contrast, a superconducting layer in 2DES would have depth dependence of superconducting parameters, such as the superconducting gap and the α and β coefficients in the GL equation, since the charge carrier density has depth dependence. We found that the angular dependence of B_{c2} well follows the GL equation in an isotropic superconductor, in spite of the change of the carrier distribution with gate bias. In addition, d_{super} is almost constant, indicating almost unchanged $(\sqrt{B_{c2}^{\perp}})/B_{c2}^{//}$ with variation of carrier distribution. Further theoretical studies are necessary for elucidating superconductivity in 2DES.

Finally, we refer to the electric field control of the $LaAlO_3/SrTiO_3$ interface with a back gate, where a domelike variation of T_c with V_G is observed [3]. Although the carrier doping mechanism of the initial state (at $V_G = 0$) in this interface system is under debate, it is known that the electric field applied through the back gate modifies the inherit spin-orbit coupling interaction in the conduction channel [14], which correlates with the appearance of T_c and raises B_{c2} above the Pauli limit. To compare our system appropriately with the $LaAlO_3/SrTiO_3$ interface system with a back gate, it is necessary to analyze experimentally an EDLT combined with the back gate, which is now being developed.

IV. CONCLUSION

In conclusion, the electric-field-induced superconductivity in $SrTiO_3$ is typical of a 2D superconductivity in spite of the change of carrier density. The angular and temperature dependence of the critical field is well-described by the 2D GL theory. The thickness of the superconducting layer was found to be almost invariant with carrier density, which contradicts with the carrier density dependent thickness of an accumulation layer calculated using a triangular quantum-well model. This may be a unique nature of superconductivity in a 2DES induced by electric field-effect in incipient ferroelectric $SrTiO_3$. Further experimental and theoretical study of the peculiar two-dimensionality is required to understand surface/interface superconductivity tuned by an electric field.

ACKNOWLEDGMENTS

This work was partly supported by Grants-in-Aid for Scientific Research (Nos. 21224009, 20540343, 25000003, 24226002, and 25708039) and one on Innovative Area "Topological Quantum Phenomena" from the Ministry of Education, Culture, Sport, Science and Technology of Japan, and by Strategic International Collaborative Research Program (SICORP-LEMSUPER) from Japan Science and Technology Agency. K. M. and Y. I. are partly supported by JSPS through the Funding Program for World-Leading Innovative R&D on Science and Technology (FIRST Program).

[1] C. H. Ahn, J.-M. Triscone, and J. Mannhart, Nature (London) **424**, 1015 (2003).
[2] K. A. Parendo, K. H. Sarwa, B. Tan, A. Bhattacharya, M. Eblen-Zayas, N. E. Staley, and A. M. Goldman, Phys. Rev. Lett. **94**, 197004 (2005).
[3] A. D. Cavigria, S. Gariglio, N. Reyren, D. Jaccard, T. Schneider, M. Gabay, S. Thiel, G. Hammer, J. Mannhart, and J.-M. Triscone, Nature (London) **456**, 624 (2008).
[4] K. Ueno, S. Nakamura, H. Shimotani, A. Ohtomo, N. Kimura, T. Nojima, H. Aoki, Y. Iwasa, and M. Kawasaki, Nat. Mater. **7**, 855 (2008).
[5] J. T. Ye, S. Inoue, K. Kobayashi, Y. Kasahara, H. T. Yuan, H. Shimotani, and Y. Iwasa, Nat. Mater. **9**, 125 (2009).
[6] K. Ueno, S. Nakamura, H. Shimotani, H. T. Yuan, N. Kimura, T. Nojima, H. Aoki, Y. Iwasa, and M. Kawasaki, Nat. Nanotechnol. **6**, 408 (2011).
[7] A. T. Bollinger, G. Dubuis, J. Yoon, D. Pavuna, J. Misewich, and I. Bozovic, Nature (London) **472**, 458 (2011).
[8] T. Nojima, H. Tada, S. Nakamura, N. Kobayashi, H. Shimotani, and Y. Iwasa, Phys. Rev. B **84**, 020502 (2011).
[9] X. Leng, J. Garcia-Barriocanal, S. Bose, Y. Lee, and A. M. Goldman, Phys. Rev. Lett. **107**, 027001 (2011).
[10] X. Leng, J. Garcia-Barriocanal, B. Yang, Y. Lee, J. Kinney, and A. M. Goldman, Phys. Rev. Lett. **108**, 067004 (2012).
[11] J. T. Ye, Y. J. Zhang, R. Akashi, M. S. Bahramy, R. Arita, and Y. Iwasa, Science **338**, 1193 (2012).
[12] F. E. Harper and M. Tinkham, Phys. Rev. **172**, 441 (1968).
[13] Y. Kozuka, M. Kim, C. Bell, B. G. Kim, Y. Hikita, and H. Y. Hwang, Nature (London) **462**, 487 (2009).
[14] M. Ben Shalom, M. Sachs, D. Rakhmilevitch, A. Palevski, and Y. Dagan, Phys. Rev. Lett. **104**, 126802 (2010).
[15] N. Reyren, S. Gariglio, A. D. Cavigria, D. Jaccard, T. Schneider, and J.-M. Triscone, Appl. Phys. Lett. **94**, 112506 (2009).
[16] J. Biscaras, N. Bergeal, A. Kushwaha, T. Wolf, A. Rastogi, R. C. Budhani, and J. Lesueur, Nat. Commun. **1**, 89 (2010).
[17] T. Ando, A. B. Fowler, and F. Stern, Rev. Mod. Phys. **54**, 437 (1982).
[18] K. Ueno, H. Shimotani, Y. Iwasa, and M. Kawasaki, Appl. Phys. Lett. **96**, 252107 (2010).
[19] K. Deguchi, T. Ishiguro, and Y. Maeno, Rev. Sci. Instrum. **75**, 1188 (2004).
[20] O. N. Tufte and P. W. Chapman, Phys. Rev. **155**, 796 (1967).
[21] R. C. Neville, B. Hoeneisen, and C. A. Mead, J. Appl. Phys. **43**, 2124 (1972).
[22] A. M. Clogston, Phys. Rev. Lett. **9**, 266 (1962).
[23] J. F. Schooley, W. R. Hosler, E. Embler, J. H. Becker, M. L. Cohen, and C. S. Koonce, Phys. Rev. Lett. **14**, 305 (1965).
[24] Y. Mizohata, M. Ichioka, and K. Machida, Phys. Rev. B **87**, 014505 (2013).